Journal of Molecular Structure 1097 (2015) 87–97

Contents lists available at ScienceDirect

Journal of Molecular Structure

journal homepage: www.elsevier.com/locate/molstruc

Studies on the synthesis, structural characterization, Hirshfeld analysis and stability of apovincamine (API) and its co-crystal (terephthalic acid: Apovincamine = 1:2)

Yu-heng Ma, Shu-wang Ge, Wei Wang, Bai-wang Sun *

School of Chemistry and Chemical Engineering, Southeast University, Nanjing 210096, PR China

HIGHLIGHTS

- The hydrogen bonds between host and guest molecules have been analyzed.
- The two apovincamine molecules are unsymmetrical in co-crystal.
- The configuration of apovincamine in co-crystal changed.
- The co-crystal strategy was successfully applied, which have better physical property in stability and solubility.

GRAPHICAL ABSTRACT

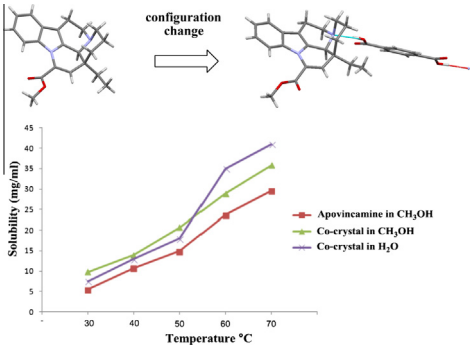

ARTICLE INFO

Article history:
Received 26 November 2014
Received in revised form 30 April 2015
Accepted 5 May 2015
Available online 15 May 2015

Keywords:
Co-crystal
Apovincamine
Hirshfeld surface
Hydrogen bond
Stability
Solubility

ABSTRACT

Apovincamine and the corresponding co-crystal have been synthesized and characterized by single crystal XRD, FT-IR, UV, TGA/DSG. Components of the crystalline phase have also been investigated in terms of their corresponding Hirshfeld surface. In the crystal lattice, a three-dimensional hydrogen-bonded network is observed in the co-crystal, including the formation of a two-dimensional molecular scaffold. Hirshfeld surfaces and fingerprint plots indicate that the structures are stabilized by H···H, C–H···π, C–H···O and O–H···N intermolecular interactions. In this work, the co-crystal strategy has been applied successfully to apovincamine. One important parameter, i.e. solubility in water, has also been significantly improved, which proves to be an important factor for bioavailability. Furthermore, DSC/TGA analysis indicates that the co-crystal maintains its crystallinity up to 200 °C, suggesting a higher stability of the co-crystal compared to apovincamine.

Introduction

In the crystalline solid state, the difference between a salt and a co-crystal is rather subtle [1,2]. This is most notably due to the unambiguous location of the hydrogen atom. Although subject to debate, generally accepted literature definitions in a broader context have been implemented: Gilli et al. [3] predicted structural parameters of salts using the strength of donor–acceptor hydrogen bonds with $\Delta pKa > 3$, whereas co-crystals where observed with $\Delta pKa < -3$. However, additional factors including the isotopic nature of the hydrogen, the crystal environment, temperature, and pressure are all influencing factors affecting the control of the proton location in the solid-state.

Traditionally focusing on salt formation [4], the formation of co-crystals has recently been developed as a potential alternative

* Corresponding author. Tel./fax: +86 25 52090614.
E-mail address: chmsunbw@seu.edu.cn (B.-w. Sun).

http://dx.doi.org/10.1016/j.molstruc.2015.05.014
0022-2860/

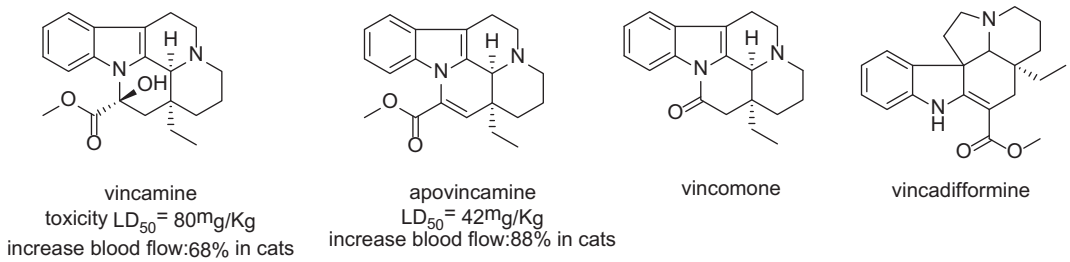

Scheme 1. Structures of alkaloids extracted from Vinca minor Linne.

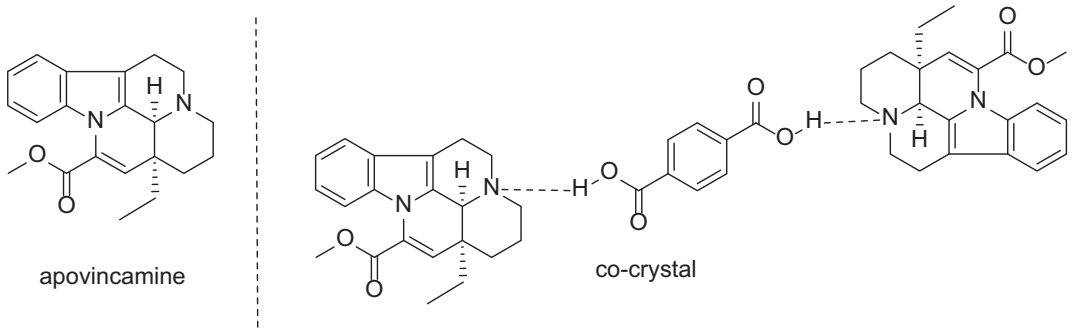

Scheme 2. The main hydrogen bonding synthons identified in the co-crystal.

Table 1
Crystal data and structure refinement for apovincamine and its co-crystal.

	Apovincamine	Co-crystal
Empirical formula	$C_{21}H_{24}N_2O_2$	$C_{50}H_{54}N_4O_8$
Formula weight	336.42	838.97
Wavelength(A)	0.71073	0.71073
Crystal system	Monoclinic	Triclinic
Space group	*P* 21	*P* 1
a (Å)	9.2278(18)	7.2450(14)
b (Å)	9.1475(18)	11.289(2)
c (Å)	10.619(2)	14.240(3)
α (°)	90	80.07(3)
β (°)	98.04(3)	78.00(3)
γ (°)	90	71.85(3)
V (Å^3)	887.5(3)	1075.3(4)
Z	2	1
T/*K*	293(2)	293(2)
Density (calculated) (g/cm^3)	1.259	1.296
Absorption coefficient (mm^{-1})	0.081	0.088
h, *k*, *l* (min, max)	(−11,11), (−11,11), (−13,13)	(0,8), (−12,13), (−16,17)
Parameters	228	565
F(000)	360	446
Goodness-of-fit on *F*2	0.993	1.039
Final *R* indices [*I*>2σ(*I*)]	*R*1 = 0.0815	*R*1 = 0.0713
	*ωR*2 = 0.1201	*ωR*2 = 0.1925
CCDC	1021467	1021468

with some of the produced co-crystals shown to display unique properties. In general, pharmaceutical co-crystals [5] are defined as multi-component crystalline structures composed of an active pharmaceutical ingredient (API) and co-crystal forming components that are solid at ambient conditions and bound via non-covalent interactions [6]. Recently, pharmaceutical co-crystals have gained a lot of attention due to their ability to tailor physiochemical properties, particularly solubility, dissolution, stability and bioavailability. With increasing popularity, the technique of co-crystallization offers the ability to design new supramolecular scaffolds with desired functional properties [7–9].

Practical applications of indole alkaloids have been employed for many years and more than 40 compound families have been isolated from plants ever since. However, the mechanism of active compounds reflected in a variety of protective and/or cognitive effects is rather complex. In the field of indole alkaloids, several target compounds [10,11] contain an eburnane skeleton, with examples including vincamine, apovincamine, vincomone and vincadifformine (Scheme 1). The latter can be extracted from Vinca minor Linne and used in a variety of medical applications, e.g. as a pharmaceutical against cerebrovascular disease [12].

In recent years much scientific attention has been devoted to the study of synthetic routes and biological activities [13] of vincamine derivatives in an effort to illustrate the further mechanisms of action and to find improved lead compounds with vasodilatory activity on cerebal blood vessels. Apovincamine has been demonstrated to exhibit particularly interesting

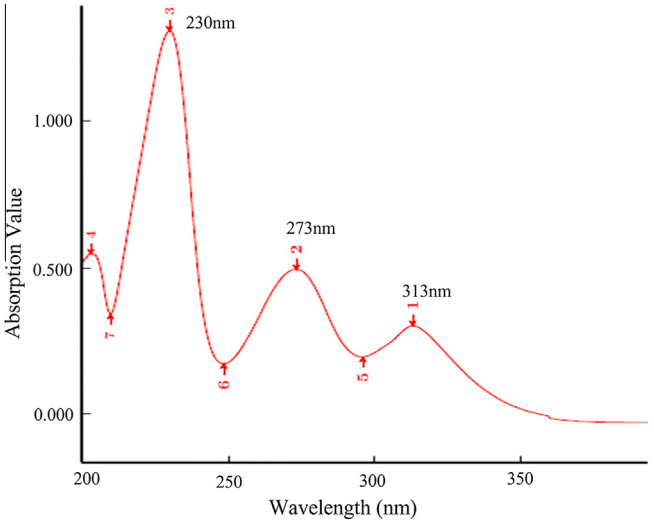

Fig. 1. The overlaid UV spectra of apovincamine.

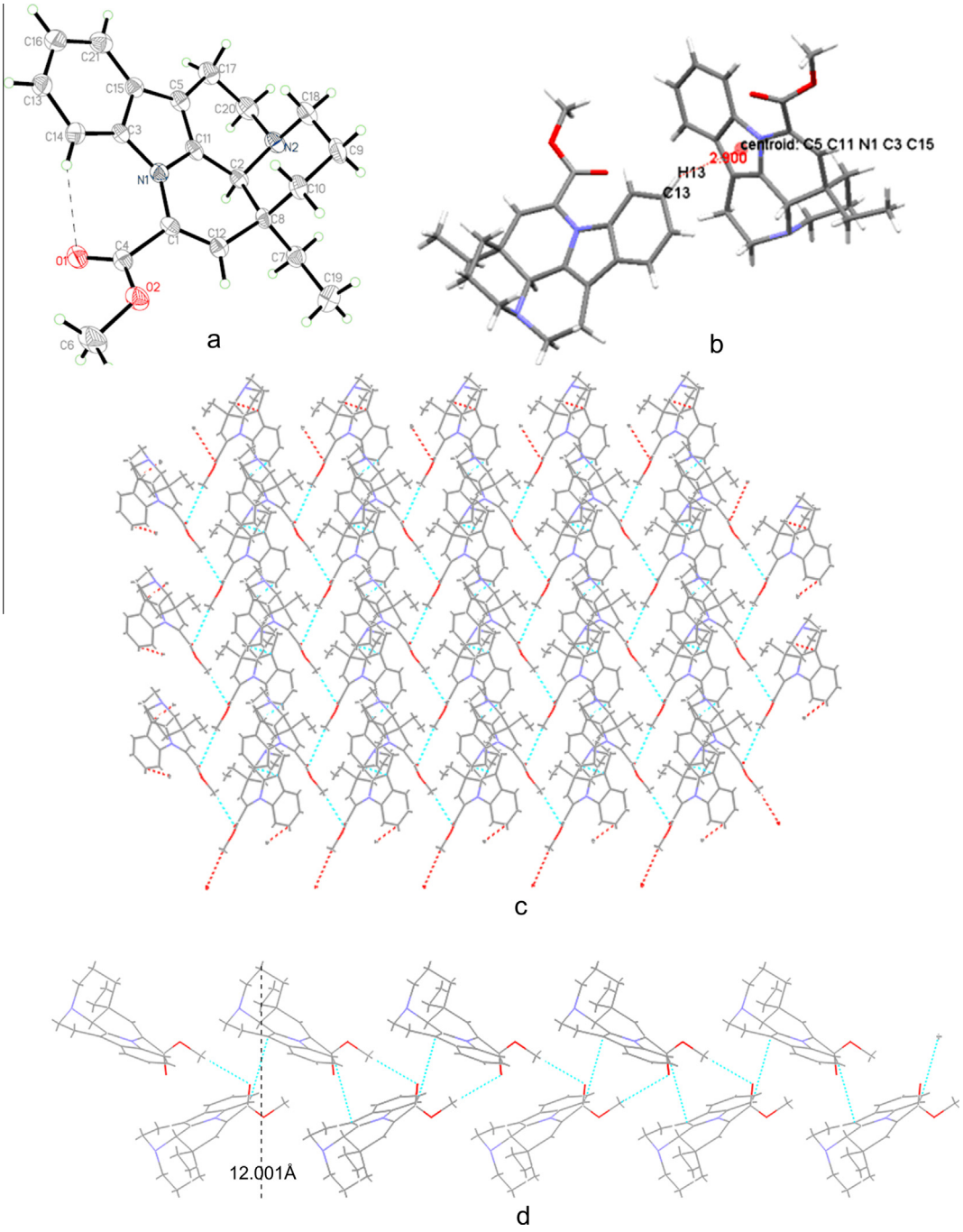

Fig. 2. Molecular structure of apovincamine, intramolecular hydrogen bonds are in dashed lines and supramolecular synthons around the $S_1^1(7)$ unit (a); crystal packing stabilized by an obvious C–H···π intermolecular interactions were observed with distance of 3.568 Å (b); a two-dimensional network viewed from *a*-axis (c); the layer structure viewed from *a*-axis with the width of 12.001 Å (d).

characteristics with an activity approximately twice that of vincamine and a hypotensive activity remaining mostly unchanged [14]. It has already been explained in great detail why the extracts show superior effects over pure vincamine.

Typically, alkaloids with widespread applications include vincamine and its derivatives. However, a general disadvantage is that these compounds show poor water solubility. The purpose of this work is to apply the co-crystal strategy to apovincamine in an effort to develop co-crystals with antioxidant features, good solubility [15] and efficient bioavailability, a feature critical to pharmaceutical applications in the treatment and/or prevention of diseases. Furthermore, to study the interaction of apovincamine with terephthalic acid, we report the synthesis and corresponding crystal structures of the co-crystals (Scheme 2). The newly synthesized apovincamine and its co-crystal were screened for solubility and stability; experimental details of these studies follow in subsequent sections.

Experimental section

General

The corresponding starting material and all reagents were obtained from commercial sources and were used without further purification. Infrared spectra were recorded on a SHIMADZU IR

Table 2
Geometrical parameters for the hydrogen bonds and C–H···π interactions in apovincamine and its co-crystal.

	D–H···A	D–H (Å)	H···A (Å)	D···A (Å)	<D–H···A (deg)	Symmetry code
Apovincamine	Inter C14–H14···O1	0.93	2.58	3.100 (5)	116	
Co-crystal	O2–H2···N2	0.82	1.80	2.592(6)	162	$1+x,y,-1+z$
	O3–H3···N4	0.82	1.8	2.603(6)	168	$x,1+y,z$
	C9–H9···O5	0.93	2.54	3.471(3)	175	
	Inter C14–H14···O2	0.93	2.45	2.759(5)	100	
	C19–H19···O9	0.93	2.54	3.464(6)	173	
	C42–H42A···O2	0.97	2.4	3.338(4)	164	$-1+x,y,1+z$
	C48–H48b···O3	0.97	2.3	3.241(3)	164	$1+x,y,-1+z$
	C–H···π		H···Cg	X···Cg	X–H···Cg	Symmetry code
Apovincamine	C13–H13···Cg(1)[a]		2.90	3.568(5)	130	$1-x,1/2+y,1-z$
Co-crystal	C14–H14···Cg(27)[b]		2.88	3.521(3)	127	$1+x,1+y,-1+z$
	C28–H28···Cg(23)[c]		2.70	3.418(2)	134	$1+x,1+y,-1+z$
	C49–H49B···Cg(27)[b]		2.76	3.514(5)	136	$-1+x,y,z$
	C53–H53A···Cg(1)[d]		2.94	3.776(4)	146	$-1+x,y,z$

[a] 6-Membered Ring N(1) → C(3) → C(15) → C(5) → C(11).
[b] 6-Membered Ring C(20) → C(21) → C(50) → C(40) → C(52) → C(38).
[c] 5-Membered Ring N(1) → C(2) → C(27) → C(21) → C(20).
[d] 6-Membered Ring N(3) → C(1) → C(3) → C(7) → C(11) → C(30).

prestige-21 FTIR-8400S spectrometer in the spectral range 400–4000 cm^{-1}, with all samples analyzed in potassium bromide pellets. Differential scanning calorimetry (DSC) and thermo gravimetric analysis (TGA) were performed using a Mettler-Toledo TGA/DSC STAR^e system at a heating rate of 10 $Kmin^{-1}$ under a dry N_2 atmosphere and at a constant flow (20 cm^3/min) over a range from 40 °C to 500 °C. Samples were placed in open aluminum oxide crucibles, annealed to 1100 °C. The TGA/DSC data were analyzed using STAR^e software provided by Mettler-Toledo. LC–MS analysis was performed on a TSQ Quantum Ultra AM LC-MS (Thermo Finnigan) with an electrospray ionization source and operated in the positive (ESI^+) mode at 350 °C with N_2 as nebulizer. The source temperature was kept at 150 °C and the capillary voltage was maintained at 5.0 kV.

Preparation of apovincamine and its corresponding co-crystal [16,17]

A mixture of vincamine (10 g, 28.2 mmol), p-toluenesulfonic acid monohydrate (10.7 g, 56.3 mmol) in 100 ml of toluene was refluxed for 2 h. During this period, any water formed in the reaction was removed by azeotropic distillation using a Marcusson trap. The progress of the reaction was monitored by thin layer chromatography (TLC). When the starting materials could no longer be detected, the solution was cooled to room temperature and evaporated *in vacuo*. The dry residue was dissolved in water and the pH was adjusted to 8 with 5% aqueous sodium hydroxide solution. After one hour, the separated material was filtered, washed with 5 ml of ethanol, and dried *in vacuo* to obtain apovincamine (8.6 g, 90%) as a white solid. ^{1}H NMR (500 MHz, $CDCl_3$): δ1.00 (m, 4H), 1.39 (m, 1H), 1.50 (d, J = 15 Hz 1H), 1.72 (m, 1H), 1.87 (m, 2H), 2.50 (m, 1H), 2.60 (t, J = 10 Hz 2H), 2.99 (m, 1H), 3.23 (m, 1H), 3.34 (dd, J = 5 Hz 1H), 3.95 (s, 1H), 4.15 (s, 1H), 6.13 (s, 1H), 7.11 (m, 1H), 7.14 (m, 1H), 7.21(m, 1H), 7.45(m, 1H); ^{13}C NMR (500 MHz, $CDCl_3$): δ8.692, 16.360, 20.285, 27.307, 28.615, 37.746, 44.922, 51.491, 52.465, 55.772, 76.751, 77.006, 77.260, 108.699, 112.414, 118.239, 120.259, 121.958, 128.144, 128.202 129.064, 134.107, 163.854; MS (ESI): required for $C_{21}H_{26}N_2O_2$ $[M]^-$,337.4; found 337.2.

The experimental procedure to obtain single crystals of apovincamine is as follows: apovincamine (1 mmol, 338 mg) was dissolved in 50 ml acetone; the solution was stirred for 1 h, filtered and the solvent was allowed to slowly evaporate under ambient conditions, yielding colorless crystals (Mp: 165.5 °C and IR, KBr pellet, cm^{-1}: 3428, 2933, 1727, 1631, 1454, 1280, 1205, 1080, 833, 744, 578, 532, 503, 468, 431).

A general experimental procedure for obtaining co-crystal is as follows: apovincamine (1 mmol, 338 mg) and terephthalic acid (0.05 mmol, 83 mg) were dissolved in 50 ml methanol; the solution was stirred for one hour, filtered and the solvent was allowed to slowly evaporate under ambient conditions to yield colorless crystals (Mp: 197.0 °C and IR, KBr pellet, cm^{-1}: 3421, 2962, 1726, 1641, 1457, 1257, 1085, 736, 642, 611, 590, 572, 559, 538, 507, 474, 431).

X-ray crystallographic studies

Single crystal X-ray diffraction data was collected at 293 K using graphite monochromated Mo Kα radiation (λ = 0.071073 nm) on Rigaku's SCX mini diffractometer with the ω-scan technique. The lattice parameters were integrated using vector analysis and refined from the diffraction matrix. Absorption corrections were carried out using the Bruker SADABS program with multi-scan method. A summary of crystallographic data, data collection, and refinement parameters is summarized in Table 1. The structural determination was carried out using the SHELX package. The structures were solved by direct method, with refinements being carried out by full-matrix least-square on $|F|^2$ using the SHELXL-97 program [18,19]. Reliability factors were defined as $R_1 = \Sigma_w(|F_0|-|F_c|)/\Sigma|F_0|$ and the function minimized was $R_w = [\Sigma_w(F_0^2-F_c^2)^2/w(F_0)^4]^{1/2}$, whereas in the least-squares calculation the unit weight was used. All non-hydrogen atoms were refined anisotropically and hydrogen atoms were inserted at their calculated positions and fixed at their positions. CCDC [20] reference numbers 1021467 and 1021468 contain the supplementary crystallographic data reported in this paper as CIF files. These data sets can be obtained free of charge from The Cambridge Crystallographic Data Centre via www.ccdc.cam.ac.uk/data_request/cif.

Hirshfeld surface calculations

Calculations of Molecular Hirshfeld surfaces [21,22] were performed using the CrystalExplorer program. When the CIF files were entered into the CrystalExplorer program, all bond lengths to hydrogen were automatically modified to typical standard neutron values [23] (C–H = 1.083 Å, N–H = 1.009 Å and O–H = 0.983 Å). All Hirshfeld surfaces were generated using a standard (high) surface resolution [24]. For a given crystal structure and a set of spherical atomic electron densities, the Hirshfeld surface is unique. The d_{norm}

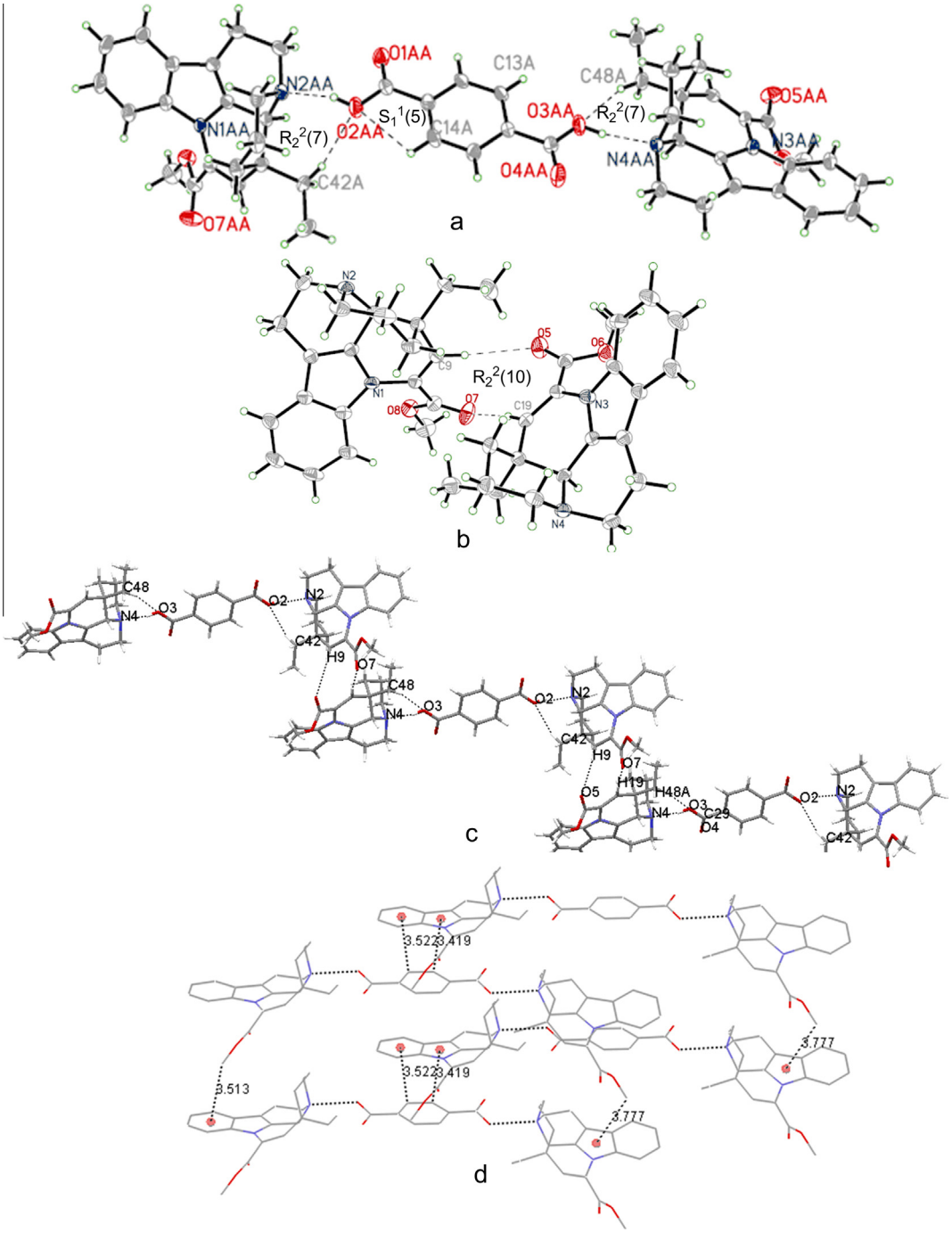

Fig. 3. Molecular structure of co-crystal, the thermal ellipsoid plot at 30% probability and hydrogen bonds between apovincamine molecules and terephthalic acid molecules (a); hydrogen bonds formed by two apovincamine molecules and supramolecular synthons around the $R_2^2(10)$ dimeric unit (b); an infinite 1D chain motif of a layer viewed from *a*-axis (c); crystal packing stabilized by an obvious C–H···π intermolecular interactions were observed with distance of 3.514 Å, 3.521 Å, 3.418 Å and 3.776 Å (d).

values [25] were mapped onto the Hirshfeld surface by employing a red–blue–white color scheme: red regions represent closer contacts and a negative d_{norm} value; blue regions represent longer contacts and a positive d_{norm} value; white regions represent the distance of contacts exactly corresponding to the Van der Waals separation with a d_{norm} value of zero. The 3-D d_{norm} surfaces can be resolved into 2-D fingerprint plots, analyzing all of the intermolecular contacts at the same time to quantitatively summarize [26,27] the nature and type of all intermolecular contacts experienced by the molecules in the crystal.

Solubility studies

An Agilent 1260 HPLC system was used to analyze apovincamine and its co-crystal, together with a 1260 variable wavelength detector (VWD). Before this procedure, an Agilent Eclipse plus-C18 analytical column (4.6 mm × 150 mm, 3.5 μm particle sizes) was used as a separation column. For apovincamine, the UV detector was set to a wavelength of 273 nm in order to avoid any interference from near ultraviolet radiation. The corresponding spectrum is shown in Fig. 1.

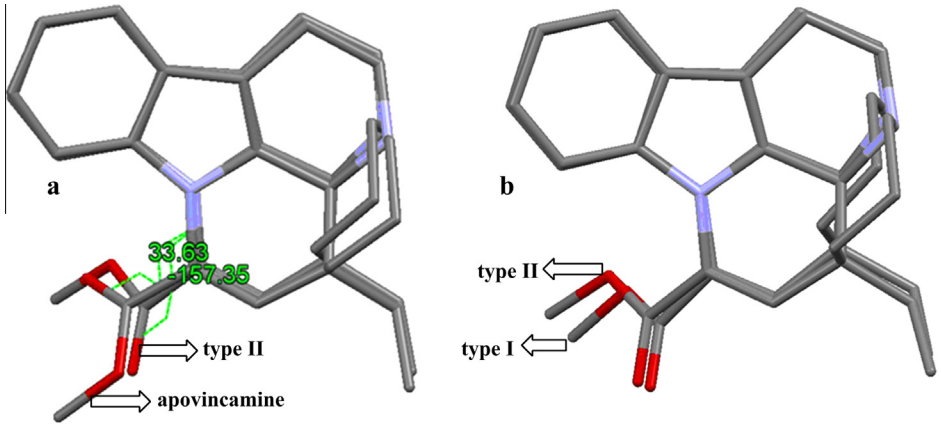

Fig. 4. The terephthalic acid induced configuration change (a); apovincamine molecules (type I and type II) have similar configuration.

A mixture of triethylamine 0.5% (pH = 7.5) and methanol (40:60) was used as the mobile phase. The column temperature was maintained at 25 °C during analysis. Pre-treatment and concentration columns were operated at ambient temperature. Pumps 1 and 2 were used to deliver mobile phase 1 at a flow rate of 0.40 ml/min and mobile phase 2 at a flow rate of 0.60 ml/min, respectively. The entire solution was filtered using a 0.45 μm membrane filter (Millipore Corp., Bedford) and degassed before performing HPLC analysis. The system was running at a flow rate of 1 ml/min and the total time was 60 min. The injection volume was 10 μl.

Stability

The degradation studies of apovincamine and the corresponding co-crystal were carried out under acid/base hydrolysis and conditions of oxidative stress according to methods previously published [28–30]. For acid hydrolysis of drug substances, solutions of apovincamine and its co-crystal were treated with 0.1 M hydrochloric acid in a water bath at 65 °C for 2 h. Alkaline hydrolysis was conducted using 0.1 M sodium hydroxide at 65 °C for 2 h. For studies on oxidative stress, sample solutions in 3% hydrogen peroxide were kept at 65 °C for 2 h. After degradation, the acidic and alkaline solutions were neutralized by adding proper amounts of sodium hydroxide or hydrochloric acid which were diluted with solvent to yield a concentration of 10 μg per ml.

Results and discussion

Crystal structures

Apovincamine crystallizes as colorless cuboid-shaped crystals, representing the P21 space group of a monoclinic system. A schematic ORTEP-drawing of apovincamine with thermal ellipsoids at 30% probability is shown in Fig. 2a. A strong intramolecular C14–H14···O1 hydrogen bond (distance of 3.100 Å and angle of 116°) can be detected forming a cyclic $S_1^1(7)$ system. C–H···π intermolecular interactions have been observed with the distance of 3.568 Å (Fig. 2b), exhibiting crucial parameters for the formation of a network structure. When viewed from the *a*-axis, a two-dimensional network is observed in this crystal lattice and

Table 3
Geometry parameters of selected bond angle and torsion angle in apovincamine and its co-crystal.

Apovincamine		Apovincamine (type II)		Apovincamine (type I)	
Bond length(Å)					
O2–C6	1.454(6)	O6–C53	1.445(9)	O8–C49	1.437(9)
C8–C12	1.515(6)	C25–C19	1.505(8)	C26–C9	1.534(8)
C5–C17	1.519(6)	C7–C41	1.509(8)	C27–C44	1.494(8)
N2–C18	1.480(6)	N4–C36	1.485(8)	N2–C43	1.503(9)
C18–C9	1.525(6)	C36–C47	1.531(9)	C43–C37	1.504(10)
C10–C8	1.552(6)	C34–C25	1.560(8)	C15–C26	1.550(9)
C8–C7	1.566(6)	C25–C48	1.534(7)	C26–C42	1.537(8)
Bond angle (°)					
C6–O2–C4	117.1(4)	C53–O6–C31	116.1(5)	C49–O8–C18	114.8(5)
C12–C1–N1	119.8(4)	C19–C35–N3	118.1(5)	C9–C23–N1	119.8(5)
C11–C5–C17	119.3(5)	C1–C7–C41	120.7(5)	C2–C27–C44	122.1(5)
N2–C2–C11	109.2(4)	N4–C12–C1	107.8(4)	N2–C3–C2	106.7(4)
C8–C7–C19	115.8(4)	C25–C48–C46	117.2(5)	C26–C42–C54	115.4(6)
Torsion angle (°)					
O2–C4–C1–C12	41.8(6)	O6–C31–C35–C19	−144.9(5)	O8–C18–C23–C9	−144.9(6)
O1–C4–C1–N1	33.7(7)	O5–C31–C35–N3	−157.4(6)	O7–C18–C23–N1	−157.1(6)
C11–C2–C8–C12	42.8(5)	C1–C12–C25–C19	45.3(6)	C2–C3–C26–C9	46.3(6)
C2–C8–C12–C1	−31.1(6)	C12–C25–C19–C35	−33.5(7)	C3–C26–C9–C23	−34.3(7)
C8–C12–C1–N1	2.8(7)	C25–C19–C35–N3	0.5(8)	C26–C9–C23–N1	0.8(8)
C12–C1–N1–C11	12.8(6)	C19–C35–N3–C1	20.1(8)	C9–C23–N1–C2	19.5(8)
C17–C20–N2–C2	64.0(5)	C41–C17–N4–C12	65.4(7)	C44–C33–N2–C3	66.6(7)
C2–N2–C18–C9	−49.6(5)	C12–N4–C36–C47	53.6(6)	C3–N2–C43–C37	53.3(6)
C10–C8–C7–C19	55.3(6)	C34–C25–C48–C46	45.8(8)	C15–C26–C42–C54	47.5(8)
C12–C8–C7–C19	−66.8(5)	C19–C25–C48–C46	−75.6(8)	C9–C26–C42–C54	−74.2(8)

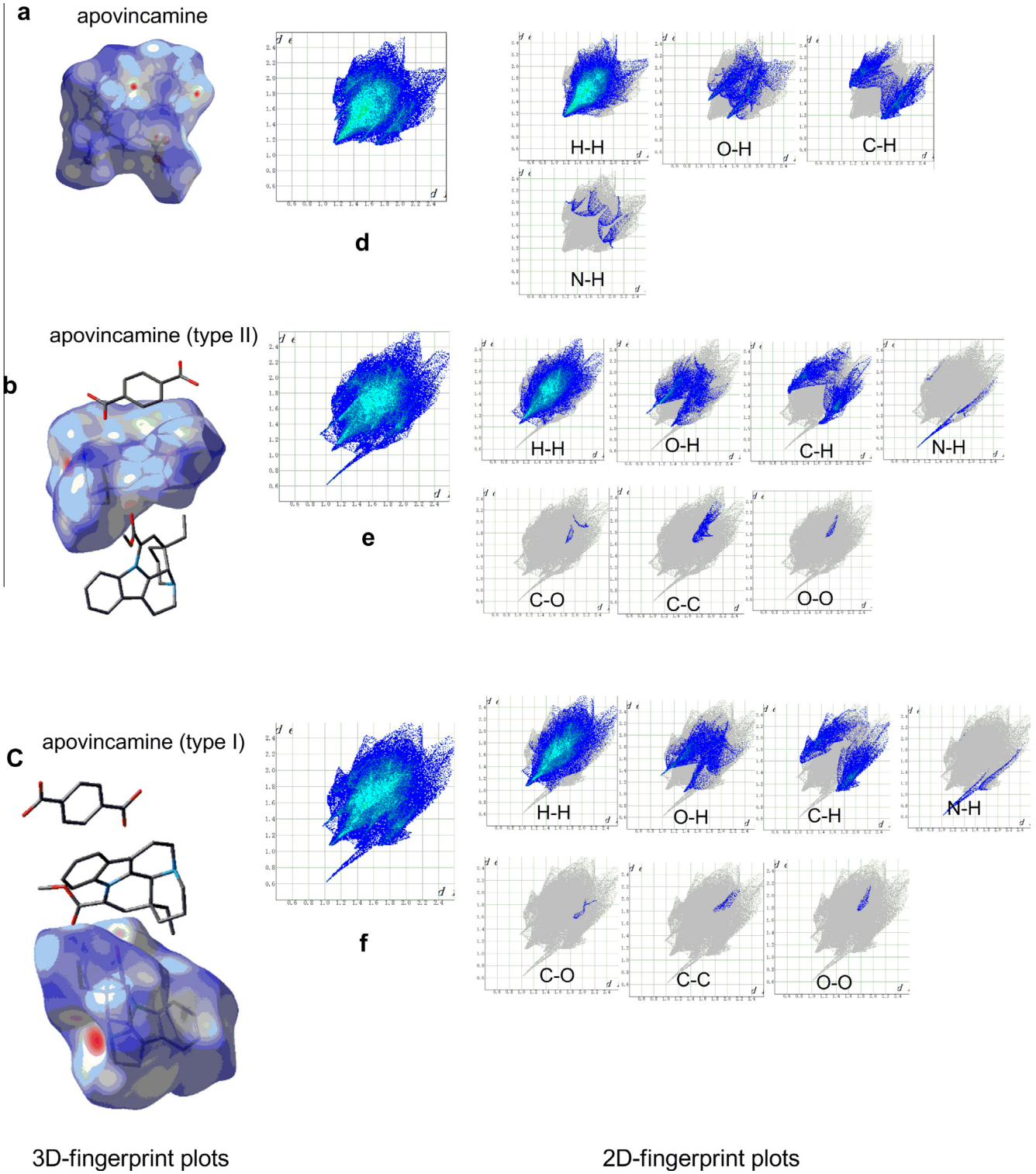

Fig. 5. 3-D d_{norm} surfaces and 2-D fingerprint plots of apovincamine molecule in two crystals.

the width of the layer is 12.001 Å (Fig. 2c and d). Geometrical parameters for hydrogen bonds present in apovincamine and its co-crystal are summarized in Table 2.

The co-crystals also form as colorless cuboid-shaped crystals, representing the P1 space group of a triclinic system, with the asymmetric unit (ASU) consisting of one terephthalic acid molecule and two apovincamine molecules. A schematic ORTEP drawing of the co-crystal with thermal ellipsoids at 30% probability was shown in Fig. 3a, in which the terephthalic acid molecule functions as a bridge connecting two apovincamine units through O–H···N and C–H···O hydrogen bonds. The apovincamine molecule (type I) and the terephthalic acid molecule formed a dimeric unit by R_2^2 (7) supramolecular heterosynthon through O–H···N (distance of 2.592 and angle of 162°) and C–H···O (distance of 3.338 Å and angle of 164°) hydrogen bond interactions. The apovincamine molecule (type II) also formed a dimeric unit by R_2^2 (7)

Table 4
Summary of the various contact contributions to apovincamine molecules in Hirshfeld surface area.

	Apovincamine (%)	Apovincamine (type II) (%)	Apovincamine (type I) (%)
H–H	67.7	63.2	62.5
H–O	12.5	17.4	17.7
C–H	17.4	15.4	17.6
N–H	2.2	1.6	1.5
C–O		0.3	0.2
C–C		1.9	0.3
O–O		0.2	0.2

supramolecular heterosynthon through O–H···N (distance of 2.603 and angle of 168°) and C–H···O (distance of 3.241 Å and angle of 164°) hydrogen bond interactions. Notable is the fact that these two pairs of C–H···O and O–H···N hydrogen bonds are almost identical and not centrosymmetric.

Further analysis reveals that the terephthalic acid molecule formed a S_1^1 (5) ring through C14–H14···O2 (distance of 2.759 and angle of 100°) hydrogen bond interactions. However, between C13–H13 and O3, no intramolecular hydrogen bond can be detected. The two apovincamine molecules form a dimeric unit by R_2^2 (10) supramolecular heterosynthon through C9–H9···O5 (distance of 3.471 Å and angle of 175°) and C19–H19···O7 (distance of 3.464 Å and angle of 173°) hydrogen bond interactions (Fig. 3b). In this crystal lattice, a three-dimensional network can be observed, which proves to be different from the two-dimensional network in apovincamine. When viewed from the *a*-axis, trimeric units display an infinite 1D chain (Fig. 3c); the 1D chain stacked across from each other and along the bc plane; C–H···π intermolecular interactions were observed with distances of 3.514 Å, 3.521 Å, 3.418 Å and 3.776 Å, respectively (Fig. 3d).

Upon overlay of the three-dimensional structures of the apovincamine molecules (Fig. 4), e.g. apovincamine-API and the apovincamine molecule (type I and type II), we found that the apovincamine molecules in the co-crystal maintain a similar configuration, not consistent with the apovincamine structure. For example, the torsion angle (O5–C31–C35–N3) is found to be −157.35°, different from the torsion angle in apovincamine (33.63°). Geometry parameters of selected bond angle and torsion angle in apovincamine and its co-crystal are provided in Table 3.

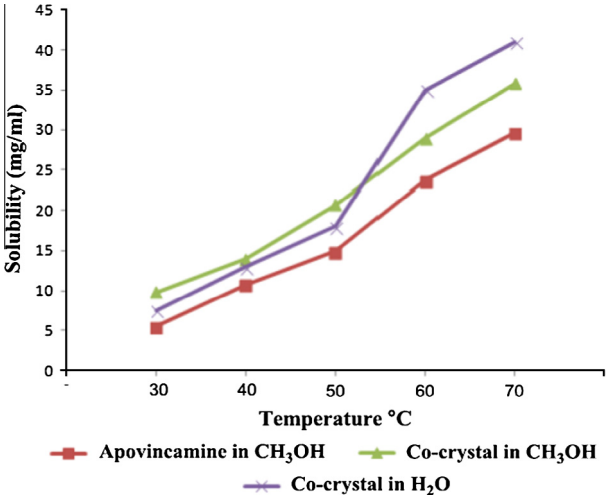

Fig. 7. Solubility of apovincamine and its co-crystal at different temperature.

Hirshfeld surface analysis

The 3D Hirshfeld surfaces of apovincamine molecules in apovincamine and its co-crystal are shown in Fig. 5a–c; they clearly show the influences of co-formers on the intermolecular interactions of the apovincamine molecule. The large and deep red spots on the 3D Hirshfeld surfaces indicate the close-contact interactions, mainly responsible for the corresponding hydrogen bond contacts. The small red spots on the surfaces represent the C–H···π interactions. The 2-D fingerprint plots are shown in Fig. 5d–f, illustrating the breakdown of 2-D fingerprint plots. With the help of these analysis results, different interactions can be separated from each other that would commonly overlap in full fingerprint plots.

For apovincamine (Fig. 5d), the H···H interactions, which are reflected in the middle of scattered points in the 2D fingerprint plots, exhibit the most significant contribution (67.7%) to the total

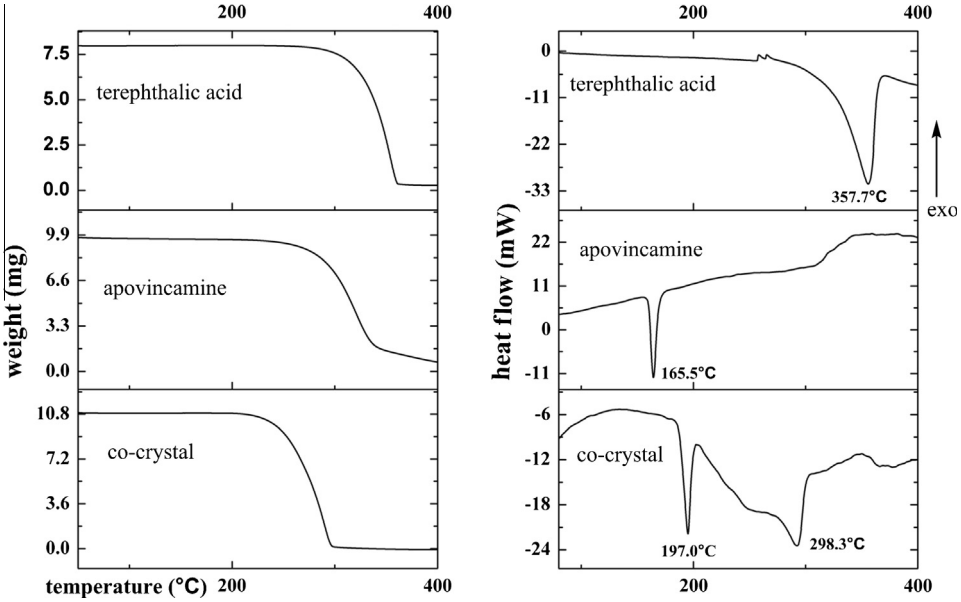

Fig. 6. The DSC and TGA profiles of apovincamine and its co-crystal.

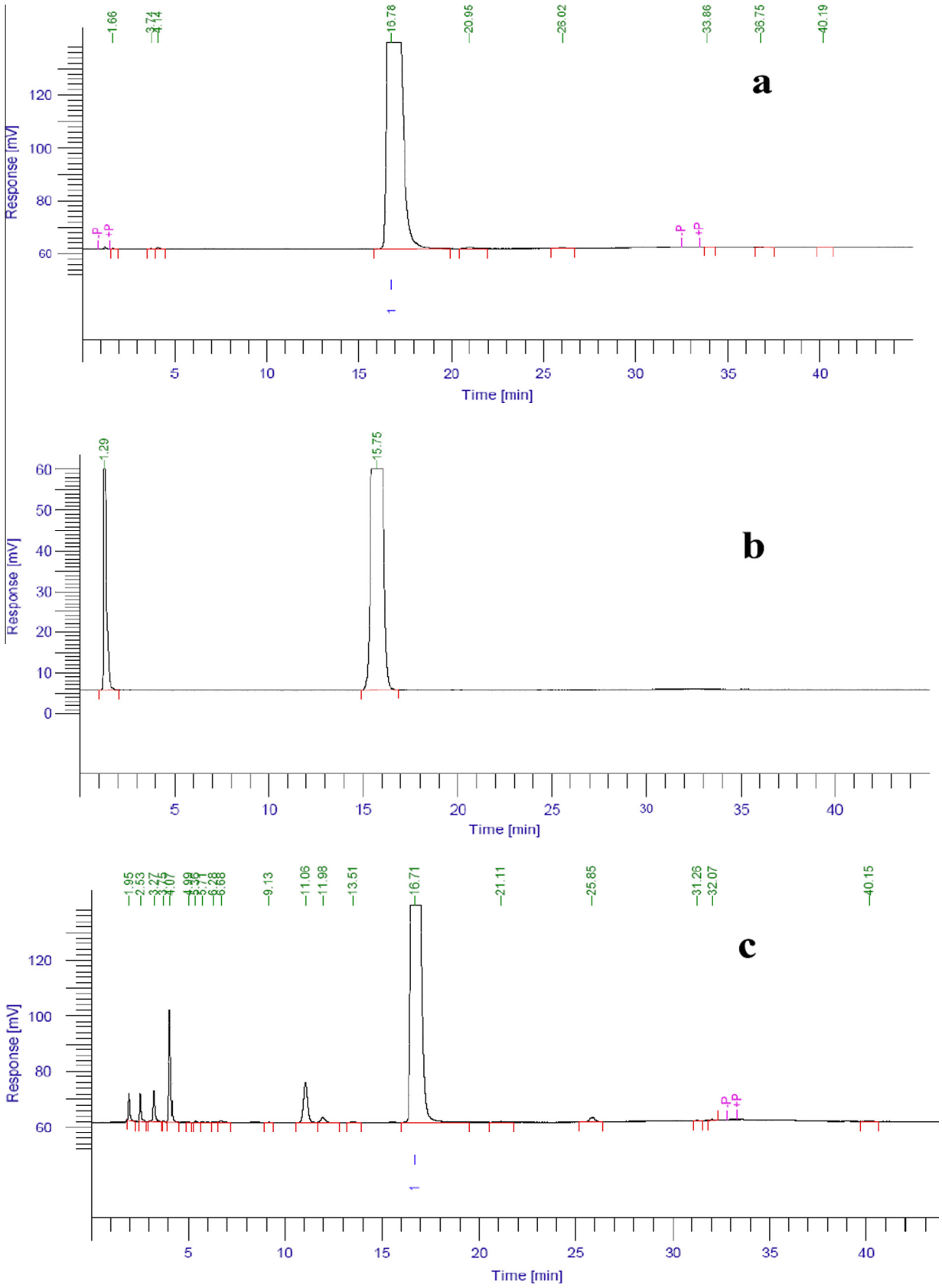

Fig. 8. Chromatogram of apovincamine under different: untreated (a); alkaline hydrolysis (b); oxidation (c).

Hirshfeld surfaces. The C–H···O hydrogen bonding intermolecular interactions appear as two very short spikes in the 2D fingerprint plots, contributing 12.5%to the total Hirshfeld surfaces. The C–H···π interactions also display a relatively large contribution to the total Hirshfeld surfaces of apovincamine, totaling 17.4%. The O–H···N hydrogen bonding interactions did not exhibit significant

contributions in the 2D fingerprint plots and merely comprise of 2.2% of the total Hirshfeld surfaces. Apart from these main interactions described above, C–C, C–O and O–O interactions were not observed, see summarized values in Table 4.

The two types of apovincamine molecules (Fig. 5e and f) display structurally similar shapes and therefore show similar intermolecular contacts. For the apovincamine molecule (type II), the H···H interactions also reflect the most significant contribution to the total Hirshfeld surfaces, totaling 63.2%. The O–H···N hydrogen bonding interaction display the second largest contribution to the total Hirshfeld surfaces, slightly larger than that in apovincamine, totaling 17.4%. The third largest contribution can be found for the C–H···π interactions, totaling 15.4%. For the apovincamine molecule (type I), the H···H, O–H···N and C–H···π followed the same order as the apovincamine molecule (type II), resulting in 62.5%, 17.7% and 17.6%. Although the two types of the apovincamine molecules are very similar, minor differences can nevertheless be found in the C–H···π and hydrogen bonds.

Further analysis of three types of the apovincamine molecules revealed an interesting phenomenon: the distance of the C–H···π interactions corresponding to their corresponding Hirshfeld surface area contributions follow the order apovincamine (type II, 3.514 Å and 15.4%) < apovincamine (API, 3.568 Å and 17.4%) < apovincamine (type I, 3.776 Å and 17.6%).

Differential scanning calorimetry (DSC) and thermogravimeric analysis (TGA)

The DSC and TGA curves of terephthalic acid, apovincamine and its corresponding co-crystal in a nitrogen atmosphere at a heating rate of 10 K min^{-1} with a temperature range of 40–400 °C are shown in Fig. 6. For terephthalic acid, the DSC curve shows an intense endothermic peak at 357.7 °C, with a sublimation enthalpy of 532.3 Jg^{-1}. For apovincamine, the melting temperature is approximately 165.5 °C, with a melting enthalpy of 77.61 Jg^{-1}. The TGA curve shows a continued weight loss from 180 °C to 400 °C with an endothermic enthalpy of 88.47 Jg^{-1}. This can be attributed to the structural decomposition of the apovincamine molecules. For the co-crystal on the other hand, the TGA curve shows two endothermic peaks. When the co-crystal begins to display a weight loss, the DSC curve exhibits an endothermic peak at 197 °C with a melting enthalpy of 50.63 Jg^{-1}. Another endothermic peak appears at 298.3 °C, with a melting enthalpy of 265.31 Jg^{-1}. The results of the DSC and TGA analysis both indicate that the co-crystal maintains its relative crystallinity up to 200 °C, suggesting that the co-crystal also exhibits a better stability than apovincamine.

Solubility studies

Solubility reflects an important parameter for bioavailability estimations. High Performance Liquid Chromatography (HPLC) in general displays major advantages in terms of sensitivity and specificity and was therefore used to investigate the solubility of apovincamine and its co-crystal. Prior to solubility measurements, stock solutions of apovincamine (1 mg/ml) were prepared in methanol, together with a series of dilutions. The mobile phase has been adjusted to 0, 0.2 0.4, 0.6, 0.8 mg/ml in an effort to obtain the corresponding working standards for the preparation of the standard curve. Then, saturated solutions of apovincamine and its co-crystal were prepared and measured by HPLC. The results of the solubility measurements were obtained through the standard curve.

Using this method, the solubility of apovincamine has been determined to be 5.5 mg/ml in CH_3OH at 30 °C, while the solubility of the co-crystal in the same solvent has been determined to be 9.8 mg/ml and the solubility of pure apovincamine under the same conditions has been determined to be 7.8 mg/ml. The solubility of apovincamine and its co-crystals at different temperature are shown in Fig. 7. Additionally, we found that through the co-crystal strategy we could further improve the solubility in CH_3OH by 25%. To find use as a injectable drug and to yield maximum dosage, the solubility of apovincamine in water is a very important parameter. Neat apovincamine could not be dissolved in water, whereas the co-crystal exhibits good solubility. The co-crystal strategy could therefore be an elegant way to solve this solubility problem in a favorable fashion.

Stability studies

Both apovincamine and its co-crystal were not found to be labile to acid hydrolysis in 0.1 M HCl at 65 °C. The experimental results obtained provide direct evidence for the hypothesis that

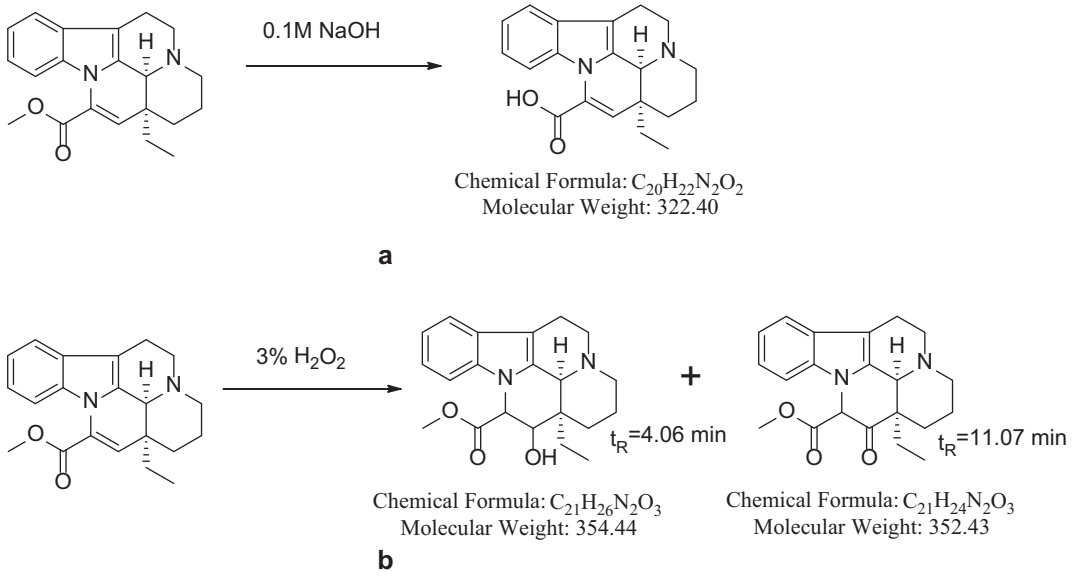

Scheme 3. The suggested pathway for the degradation in 0.1 M NaOH (a) and 3% H_2O_2 (b).

the co-crystal strategy does not reduce the stability of apovincamine. However, apovincamine and its co-crystal have been shown to be highly labile to alkaline hydrolysis: around 36.7% degradation of apovincamine has been observed in 0.1 M NaOH at 65 °C and within 2 h. The degradation peaks appeared at tR 1.29 min and similar degradation has been observed in the co-crystal (Fig. 8b). HPLC analysis revealed that the rate of degradation increased with time. The structural characteristics have been confirmed the LC–MS analyses. The mass of the degradation product was found to be m/z 323.17 $[M+H]^+$ which corresponds to the mass of apovincaminic acid. The presumed degradation pathway in 0.1 M NaOH is shown in Scheme 3a.

The co-crystal was found to be relatively stable upon exposure to oxidative conditions (e.g. 3% H_2O_2 at 65 °C for 2 h), the presence of any degradation product (>1/1000) could not be detected by HPLC. Neat apovincamine on the other hand was found to be prone to oxidation under these condition, resulting in about 10% degradation. Two major peaks corresponding to the degradation product appeared at t_R 4.06 min and 11.07 min (Fig. 8c). LC-MS analysis revealed the molecular mass of the degradation products at m/z 355.3 $[M+H]^+$ and 353.6 $[M+H]^+$. The presumed degradation pathway is shown in Scheme 3b.

Conclusions

In summary, we have presented the synthesis, crystal structure, Hirshfeld surface, IR spectra, thermal analysis (DSC and TGA) of apovincamine and its corresponding co-crystal. The results of the Hirshfeld surface and crystal structure analysis in particular offer detailed insights into the intermolecular interactions and the kinds of interactions providing significant contributions to the stability of the structures. Furthermore, the stability analysis results show that the co-crystal offers improved physical properties and a combination of theoretical and experimental methods suggest that a close connection between structure and stability can be noted. High stability tends to favor the co-crystal with more hydrogen bonds being present. Apart from the analyses described above, another relevant parameter could be improved; by employing the co-crystal strategy, the solubility in water could be improved significantly. The latter is an important factor for bioavailability and potential medical applications of this family of compounds.

Acknowledgements

This work has been supported by the prospective joint research project of Jiangsu province (BY2012193) and the Fundamental Research Funds for the Central Universities (CXZZ12_0119).

Appendix A. Supplementary material

Supplementary data associated with this article can be found, in the online version, at http://dx.doi.org/10.1016/j.molstruc.2015.05.014.

References

[1] G. Ramon, K. Davies, L.R. Nassimbeni, CrystEngComm. 16 (2014) 5802–5810.
[2] C.C. Seaton, CrystEngComm. 16 (2014) 5878–5886.
[3] P. Gilli, L. Pretto, V. Bertolasi, G. Gilli, Acc. Chem. Res. 42 (2009) 33–44.
[4] C.C. Seaton, T. Munshi, S.E. Williamsb, I.J. Scowen, CrystEngComm. 15 (2013) 5250–5260.
[5] J.W. Steed, Trends Pharmacol. Sci. 34 (2013) 185–193.
[6] P. Vishweshwar, J.A. McMahon, J.A. Bis, M.J. Zaworotko, J. Pharm. Sci. 95 (2006) 499–516.
[7] N. Blagden, S.J. Colesb, D.J. Berry, CrystEngComm. 16 (2014) 5753–5761.
[8] D. Braga, F. Grepioni, L. Maini, S. Prosperi, R. Gobetto, M.R. Chierotti, Chem. Commun. 46 (2010) 7715–7717.
[9] D. Braga, F. Grepioni, G.I. Lampronti, L. Maini, A. Turrina, Cryst. Growth. Des. 11 (2011) 5621–5627.
[10] D. Hasa, B. Perissutti, S.D. Acqua, M.R. Chierotti, R. Gobetto, I. Grabnar, C. Cepek, D. Voinovich, Eur. J. Pharm. Biopharm. 84 (2013) 138–144.
[11] Y.G. Smeyers, N.J. Smeyers, J.J. Randez, H. Laguna, E.G. Ruano, Mol. Eng. 1 (1991) 153–160.
[12] G. Lewin, C. Schaeffer, Tetrahedron Lett. 39 (1998) 9689–9692.
[13] K. Koyama, Y. Hirasawa, T. Hosoya, T.C. Hoe, K.L. Chan, H. Morita, Bioorg. Med. Chem. 18 (2010) 4415–4421.
[14] L. Kisfaludyl, L. Szporny, L. Csaba, EP, DE1958514 [P], 10 NOV 1971.
[15] N. Upadhyay, T.P. Shukla, A. Mathur, Manmohana, S.K. Jha, Int. J. Pharm. Sci. Rev. Res. 8 (2011) 144–148.
[16] B. Danieli, S. Lesma, G. Palmisano, Tetrahedron Lett. 19 (1981) 1827–1828.
[17] L. Szabb, G. Kalaus, C. SzBntay, Arch. Pharm. 316 (1983) 629–638.
[18] CrysAlis CCD and CrysAlis Red, Version 171.32.8, Oxford Diffraction Poland, Wrocław, Poland, 2006.
[19] G.M. Sheldrick, SHELXL-97, University of Gottingen, Germany, 1997.
[20] CCDC, Cambridge, U.K., 2003–2004.
[21] M.A. Spackman, J.J. McKinnon, CrystEngComm. 4 (2002) 378–382.
[22] F.L., Hirshfeld, Theor. Chim. Acta. 44 (1977) 129–133.
[23] F.H. Allen, O. Kennard, D.G. Watson, L. Brammer, A.G. Orpen, R. Taylor, J. Chem. Soc. Perkin Trans. 2 (1987) S1.
[24] J.J. McKinnon, M.A. Spackman, A.S. Mitchell, Acta Crystallogr. Sect. B 60 (2004) 627–668.
[25] S.K. Wolff, D.J. Grimwood, J.J. McKinnon, D. Jayatilaka, M.A. Spackman, CrystalExplorer 2.1, University of Western Australia, Perth, Australia, 2007.
[26] A.L. Rohl, M. Moret, W. Kaminsky, K. Claborn, J.J. Mckinnon, B. Kahr, Cryst. Growth Des. 8 (2008) 4517–4525.
[27] A. Parkin, G. Barr, W. Dong, C.J. Gilmore, D. Jayatilaka, J.J. Mckinnon, M.A. Spackman, C.C. Wilson, CrystEngComm. 9 (2007) 648–652.
[28] N.O. El'tsov, G.B. Golubitskii, E.V. Budko, J. Anal. Chem. 69 (2014) 1011–1023.
[29] A.K. Amruthraj, B.M. Venkatesha, S. Ananda, Int. J. Pharm. Sci. Rev. Res. 11 (2014) 62–66.
[30] G. Yanamadala, P. Srikumar, Int. J. Pharm. 4 (2014) 448–457.